Biology of Reproduction, 2019, 100(1), 268–280
doi:10.1093/biolre/ioy176
Research Article
Advance Access Publication Date: 1 August 2018

OXFORD

Research Article

Electroacupuncture facilitates implantation by enhancing endometrial angiogenesis in a rat model of ovarian hyperstimulation†

Wei Chen[1], Jie Chen[2], Menghao Xu[3], Zhiyan Zhong[1], Qing Zhang[1], Wei Yang[4,*] and Guangying Huang[1,*]

[1]Institute of Integrated Traditional Chinese and Western Medicine, Tongji Hospital, Tongji Medical College, Huazhong University of Science and Technology, Wuhan, Hubei, China; [2]Department of Biochemistry and Molecular Biology, Tongji Medical College, Huazhong University of Science and Technology, Wuhan, Hubei, China; [3]School of Basic Medicine, Tongji Medical College, Huazhong University of Science and Technology, Wuhan, Hubei, China and [4]Reproductive Medicine Center, Tongji Hospital, Tongji Medicine College, Huazhong University of Science and Technology, Wuhan, Hubei, China

*__Correspondence:__ Wei Yang, Reproductive Medicine Center, Tongji Hospital, Tongji Medicine College, Huazhong University of Science and Technology, 1095 Jiefang Avenue, Wuhan, Hubei 430030, China. Tel: +86-13507160909; E-mail: zqq_vivi@126.com; Guangying Huang, Institute of Integrated Traditional Chinese and Western Medicine, Tongji Hospital, Tongji Medical College, Huazhong University of Science and Technology, Wuhan, Hubei 430030, China. E-mail: gyhuang@tjh.tjmu.edu.cn

†__Grant Support:__ This study was funded by National Natural Science Foundation of China (NSFC) (81202827).
Edited by Dr. Haibin Wang, PhD, Xiamen University

Received 22 February 2018; Revised 6 July 2018; Accepted 31 July 2018

Abstract

Controlled ovarian hyperstimulation (COH) impairs the synchronized development of endometrium and embryo, resulting in the failure of embryo implantation. Here, we investigated what effects electroacupuncture had on embryo implantation in COH rats. Female rats were randomly assigned to four groups: normal (N), model (M), electroacupuncture (EA), and electroacupuncture pretreatment (PEA). Rats in groups M, EA, PEA were injected with pregnant mare serum gonadotropin (PMSG) and human chorionic gonadotropin to establish the COH model. Rats in group EA received electroacupuncture treatment from the PMSG injection day to the 3rd day of pregnancy (D3), while those in group PEA received electroacupuncture treatment for 3 days before the PMSG day and continuing to D3. Furthermore, another 30 female rats who received the same treatment as the rats in group PEA were injected with siVEGFR2 into uterine lumen. The endometrial microvascular density (MVD) and the expression levels of vascular endothelial growth factor-A, angiopoietin-1, and fibroblast growth factor-2 were significantly lower in groups M than in groups N and PEA. The percentage of dolichos biflorus agglutinin positive uterine natural killer cells in groups N, EA and PEA was higher than that in group M. After the siVEGFR2 injection, the protein expression levels of vascular endothelial growth factor receptor 2 (VEGFR2), PI3K, p-AKT and p-ERK, the embryo number and the MVD were significantly reduced. In conclusion, electroacupuncture can facilitate embryo implantation in COH rats by activating the VEGFR2/PI3K/AKT and VEGFR2/ERK signaling pathways which have a positive relationship with endometrial angiogenesis.

Summary Sentence

Electroacupuncture can facilitate embryo implantation in COH rats by activating the VEGFR2/PI3K/AKT and VEGFR2/ERK signaling pathways which have a positive relationship with endometrial angiogenesis.

Key words: electroacupuncture, implantation, angiogenesis, endometrial receptivity, controlled ovarian hyperstimulation, signaling pathway.

Introduction

In vitro fertilization-embryo transfer (IVF-ET) treatment is currently widely applied in assisted reproductive technology (ART). As an important measure to achieve a sufficient number of oocytes, controlled ovarian hyperstimulation (COH) is applied in IVF-ET treatment. However, the development of ovarian hyperstimulation syndrome (OHSS) is the most common complication in IVF-related ovarian stimulation [1]. The high or rapidly rising serum estradiol (E2) level after ovarian hyperstimulation could lead to implantation defects and improper decidualization [2, 3]. Furthermore, ovarian hyperstimulation in rats causes a dysregulation in uterine fluid dynamics which results in an unfavorable implantation environment for the blastocyst [4]. As a result, the clinical pregnancy and implantation rates are still no more than 50% and 30%, respectively, in the cycle of IVF-ET [5–8]. The success of IVF-ET depends on three factors: a high-quality embryo, a maternal endometrium with relatively good receptivity, and the synchronization of the embryo and endometrial development [9, 10].

Endometrial receptivity is the ability of the maternal endometrium to allow the blastocyte to adhere and penetrate to achieve successful embryo implantation. Endometrial receptivity is dramatically reduced upon stimulation in ART which results in lower pregnancy rate [11]. Angiogenesis plays an important role in embryo implantation, and its failure limits the achievement of a successful outcome in ART [12]. The formation of the placenta can be restrained by certain angiogenesis inhibitors, and this may cause embryo resorption [13]. Furthermore, during the midsecretory period, the high coexpression of the vascular endothelial growth factor receptor 1 (VEGFR1) and VEGFR2 in microvessels accompanied with increased microvascular density (MVD) and vascular permeability is a prerequisite for implantation [14]. In this sense, angiogenesis determines whether an embryo can survive during the peri-implantation period and is presumed to be one of the most important standards for evaluating endometrial receptivity.

In rats, implantation usually occurs during a brief 24-h period, 5 days after mating. This period is considered the "implantation window" (IW), and during this period endometrium achieves a status that allows the zygote to adhere [9, 15]. However, prior to or after the IW, it is difficult for the blastocyst to attach to the endometrium [16]. Hence, desynchronized development of the embryo and endometrium can lead to implantation failure.

Acupuncture, also called traditional acupuncture or manual acupuncture, has been applied for thousands of years to relieve patients from diseases. Previous studies found that acupuncture can be used to treat implantation failure [17–19] and can remodel microvessels and regulate the immune microenvironment in the endometrium, which is beneficial for embryo implantation [18]. Electroacupuncture is an improved and developed therapeutic method based on traditional acupuncture. More recently, electroacupuncture has been used to improve endometrial receptivity in patients undergoing frozen-thawed embryo transfer [20]. Also, electroacupuncture could improve the IVF outcomes [21]. Therefore, in this study, we established a rat model of COH and examined whether electroacupuncture has any effects on angiogenesis through affecting the expression levels of vascular endothelial growth factor A (VEGF-A), angiopoietin 1 (Angpt-1) and fibroblast growth factor 2 (FGF-2) and the percentage of dolichos biflorus agglutinin positive (DBA^+) uterine natural killer (uNK) cells in the endometrium of COH rats, in such a way that improves endometrial receptivity. We also sought to identify the signaling pathways that is affected by electroacupuncture treatment in COH rats.

Materials and methods

Animals

A total of 260 SPF mature, virginal Wistar female rats aged 10–12 weeks and 30 SPF male Wistar rats aged 10–12 weeks were provided by the Center for Disease Control and Prevention of Hubei Province. We followed The Guidelines for the Care and Use of Animals in Research enforced by the Hubei Municipal Science and Technology Commission. All protocols were approved by the Institutional Review Board (IRB ID: TJ-A20160501), Tongji Hospital, Tongji Medical College, Huazhong University of Science and Technology.

Animal model

After acclimation for 1 week, 210 rats were randomly divided into eight groups: normal (N), model (M), electroacupuncture (EA), electroacupuncture pretreatment (PEA), normal+electroacupuncture (N+EA), normal+electroacupuncture pretreatment (N+PEA), electroacupuncture control (EA'), and electroacupuncture pretreatment control (PEA'). The oestrous cycle of the rats was determined by observation of vaginal smears. To establish the COH model, rats in groups M, EA, PEA, EA', and PEA' received intraperitoneal injections of 0.7 ml of pregnant mare serum gonadotropin (PMSG, 8 IU/100 g weigh, Hangzhou Animal Medicine Factory, China) at 5:00 pm during diestrus and of 0.7 ml of human chorionic gonadotropin (HCG, 16 IU/100 g weigh, Livzon Pharmaceutical Factory, Zhuhai, China) 46 h later. Rats in groups N, N+EA, and N+PEA received an intraperitoneal injection with an equal volume of phosphate-buffered saline (PBS) at the same time as the PMSG and HCG injections. All female rats were mated with male rats at a 1:1 ratio at night on the HCG day. If spermatozoa was detected in the vaginal smear on the following day, this day was defined as the first day of gestation (D1). All rats were anaesthetized with 1% pentobarbital and sacrificed on D4, D6, or D8. Embryos in part of the uterus were washed away by PBS and then the uterus was stored at −80°C.

Isoflurane anesthesia test

Twenty rats were randomly divided into four groups: normal group (N), N+Anesthesia group, model group (M), M+Anesthesia group. Rats in groups N and M were treated as mentioned in "Animal Model". Except for receiving the same treatment with the rats in groups N and M, rats in group N+Anesthesia and M+Anesthesia,

respectively, were anesthetized with 2% isoflurane (RWD Life Science lnc., Shenzhen, China) for 6 days before HCG day and 3 days after HCG day. All rats were anaesthetized with 1% pentobarbital and sacrificed on D8.

Electroacupuncture procedure

Rats in groups EA, PEA, N+EA, N+PEA, EA', and PEA' were anaesthetized with 2% isoflurane [22–25] and then treated with electroacupuncture. Sanyinjiao (SP6) and Housanli (ST36) were chosen as the acupuncture points by using an electroacupuncture stimulator instrument (HANS-200E, Nanjing, Jisheng, Jiangsu, China) in groups EA, PEA, N+EA, and N+PEA. Neiguan (PC6) and Waiguan (TE5) were chosen as the acupuncture points in groups EA' and PEA'. The locations of the acupuncture points were based on the concepts of Traditional Chinese Medicine and the homologous anatomical location in rats. SP6 is situated approximately 10 mm above the top of the medial malleolus and on the posterior border of the tibia. ST36 is located at the posterolateral border of the knee, approximately 5 mm below the capitulum fibula. PC6 is located about 3 mm above the transverse stripe of the wrist at the axopetal end. TE5 is located at the midpoint between the ulna and the radius, about 3 mm above the dorsal crease of the wrist. Four 0.18 mm germfree acupuncture needles (Human Health, Shanghai, China) were connected to the output terminal of the electroacupuncture stimulator instrument and inserted into the SP6 and ST36 or the PC6 and TE5 acupuncture points. SP6 and ST36 were inserted at a depth of 5 and 7 mm, respectively. PC6 and TE5 were both inserted at a depth of 1 mm. The stimulation frequencies were 2/15 Hz, and the intensity was determined by the muscle twitch threshold. Rats in group EA received electroacupuncture treatment for 15 min per day from the PMSG injection day to D3, while those in group PEA received electroacupuncture treatment for 3 days before the PMSG day and continuing to D3.

Injection of siRNA

Except for administering the same treatment with the rats in group PEA, another 30 rats were anaesthetized via an intraperitoneal injection of 1% pentobarbital sodium [26], and the uterus horns were visualized through an incision at dorsum of the rats at 2:00 pm on D1. A 50 μl of mixture containing 25 μl of siVEGFR2 solution (10 μM siVEGFR2, Beijing ViewSolid Biotech Co., Ltd, Beijing, China) and 25 μl of AteloGeneTM (KOKEN, Tokyo, Japan) was injected into the right uterine lumen, and a 50 μl of mixture containing 25 μl of siNC solution (10 μM si-NC, Beijing ViewSolid Biotech Co., Ltd, Beijing, China) and 25 μl of AteloGeneTM was injected into the left uterine lumen as the control. Rats were sacrificed on D4, D6, or D8 (n = 10), and uteri were preserved for the following experiments.

MVD analysis

The MVD was detected by immunohistochemistry of CD31. After being fixed and embedded in paraffin, the tissues were cut into 5-μm sections. The paraffin-embedded sections were kept at 65°C for 2 h and then dewaxed and rehydrated with xylene and degraded ethanol. After antigen retrieval with EDTA buffer, elimination of the endogenous hydrogen peroxidase and the blocking of non-specific antigens with 5% BSA (10735078001, Roche, Swiss), these sections were incubated with a goat anti-CD31 goat polyclonal antibody (1:100 dilution; sc-1506, Santa Cruz Biotechnology Inc., CA, USA) overnight at 4°C or with PBS as a negative control. After three washes with PBS, all tissues were incubated with HRP-Rabbit anti Goat secondary antibody (1:100, AS1108, ASPEN, China) for 1 h and then stained with 3, 3'-diaminobenzidine (DAB). The MVD was calculated based on the number of CD31-positive vessels viewed at 400× magnifications (40× objective lens and 10× ocular lenses) and using Image-Pro Plus 6.0 software. For each section, microvessels in at least five randomly selected fields were counted.

Electrochemiluminescence immunoassay

After the rats were anaesthetized with 1% pentobarbital, blood samples were collected from the abdominal aorta and then kept at room temperature for 20 min. After centrifuged at 3000 rpm for 15 min, the serum was obtained. The levels of serum estradiol and progesterone were determined by electrochemiluminescence immunoassay in ADVIA Centaur XP system (Siemens, Germany).

Immunofluorescence of VEGF-A, Angpt-1, and FGF-2

After dewaxed and rehydrated with xylene and degraded ethanol, the tissue sections of uteri were labeled with primary antibodies against VEGF-A (1:50, sc-7269, Santa Cruz, USA), Angpt-1 (1:50, sc-6319, Santa Cruz, USA), or FGF-2 (1:100, sc-79, Santa Cruz, USA). The sections were incubated with Cy3-Goat anti Mouse (1:50, AS1111, ASPEN, China), Cy3-Donkey anti Goat (1:50, AS1113, ASPEN), and Cy3-Goat anti Rabbit (1:50, AS1109, ASPEN) secondary antibodies the next day. Then, these sections were observed under 100× magnifications.

Western blot analysis

The endometria acquired from the uterine slices were previously stored in –80°C, and for the experiment, the samples were lysed in RIPA total protein lysis buffer (AS1004, ASPEN, China) and centrifuged at 12 000 rpm for 15 min at 4°C. Samples were resolved on 10% sodium dodecyl sulfate-polyacrylamide gel electrophoresis (SDS-PAGE) gels and were transferred to nitrocellulose membranes. The membranes were incubated overnight at 4°C with the following primary antibodies: anti-VEGF-A (1:1000), anti- Angpt-1 (1:500), anti-FGF-2 (1:500), anti-placental growth factor (PGF, 1:2000, DF6579, Affinity Biosciences, UK), anti-delta like canonical Notch ligand-1 (DLL-1, 1:500, ab10554, Abcam), anti-VEGFR-2 (1:500, ab11939, Abcam), anti-PI3K (1:2000, 3358, Cell Signaling Technology, Inc., MA, USA), anti-p-AKT (1:2000, 4060, Cell Signaling Technology), anti-AKT (1:2000, 4691, Cell Signaling Technology), anti-p-ERK (1:1000, 4370, Cell Signaling Technology), anti-ERK (1:2000, 4695, Cell Signaling Technology), anti-β-Actin (1:10000, TDY051, Beijing TDY Biotech Co., Ltd, China). After washing five times with Tris-buffered saline/Tween-20 (TBST) for 8 min per wash, the membranes were incubated with the HRP-Goat anti Rabbit (1:10000, AS1107, ASPEN), HRP-Rabbit anti Goat (1:10000, AS1108, ASPEN), and HRP-Goat anti Mouse (1:10000, AS1106, ASPEN) secondary antibodies for 30 min at room temperature. The membranes were then developed with prepared ECL solution (AS1059, ASPEN) and transferred to films (XBT-1, Kodak, USA) in the dark. The gray values were analyzed by AlphaEaseFC 4.0.

Real-time PCR analysis

Total RNA was extracted from the endometria of rats using TRIzol (Invitrogen Life Technologies, USA). Real-time PCR was performed with 1 μg of total RNA per 20-μl reaction using a standard cDNA Synthesis kit (Takara Bio Inc., Japan). Real-time PCR primer sequences are shown in Supplementary Table S1.

Typical thermal cycling conditions for each real-time PCR reaction included a holding stage at 95°C for 30 s, 40 cycles of amplification including 95°C for 5 s, and 60°C for 30 s, and a melting curve stage including 95°C for 15 s, 60°C for 1 min, and 95°C for 15 s. Real-time PCR was performed on a Step-One Real-Time PCR System (Applied Biosystems). Gene expression was analyzed using the $2^{-\Delta\Delta Ct}$ algorithm.

Flow cytometric analysis of DBA$^+$ uNK cells

Cell suspensions were generated by shredding and grinding the endometrial tissues in 3 ml of 1640 medium supplemented with 10% fetal bovine serum (Zhejiang Tianhang Biotechnology Co., Ltd, China). After filtration and centrifugation, a mixture of 4 ml of cell suspension and 4 ml of lymphocytes separation medium (Tianjin Haoyang Biological Manufacture Co., Ltd, China) was centrifuged at 1350 g for 30 min at 20°C. After washing the samples twice, the cell suspension was incubated with anti-CD32 (0.1 μl/10^6 cells in 100 μl buffer, BD Biosciences, USA) for 10 min at 4°C to block Fc receptors (FcRs). Samples were then incubated with biotin-conjugated DBA-lectin (1 μl/10^6 cells in 100 μl buffer, Sigma-Aldrich, USA) for 3 min, and the suspension was incubated with FITC-avidin (0.25 μl/10^6 cells in 100 μl buffer, BioLegend Inc., USA) for 30 min at 4°C. After the incubation period, samples were analyzed using a flow cytometer (Accuri C6, BD Biosciences, USA).

Statistical analysis

All the experimental data were presented as mean ± standard error of mean (SEM). Data were tested for normal distribution before analysis. One-way analysis of variance was used for multiple comparisons by using Statistics Package for Social Science (SPSS 19.0, USA). The LSD test was used for data with assumed equal variance, while Dunnett T3 test was used for data under the assumption of unequal variance. Statistical significance was indicated at $P < 0.05$.

Results

Embryo number and endometrial MVD

The embryos in group M were unevenly distributed compared with those in the other groups (Figure 1A). The embryo number in group M (7.50 ± 1.88) was significantly fewer than that in groups N (12.33 ± 1.15) and PEA (15.25 ± 1.41); however, there was no significant differences between groups M and EA (10.20 ± 1.24; Figure 1B). Moreover, the embryo number had no significant difference between groups N and N+Anesthesia ($P > 0.05$), and also between groups M and M+Anesthesia ($P > 0.05$, Supplementary Figure S1). These findings may indicate that anesthesia with isoflurane has no significant effect on embryo implantation in rats [27] and COH decreases the implantation rate, but PEA treatment can improve it. There was a clear reduction in the number of CD31-positive microvessels in groups M and EA compared with groups N and PEA on D4 (Figure 1C) and D6 (Figure 1D). The endometrial MVD was significantly higher in groups N and PEA than in groups M on D4 (Figure 1E) and D6 (Figure 1F). No significant difference was found between groups M and EA ($P > 0.05$, Figure 1E and F). These data may indicate that the implantation rate has a positive relation with the MVD. Moreover, the embryo numbers and MVDs had no significant differences among groups N, N+EA, and N+PEA ($P > 0.05$, Supplementary Figure S2A–F) which indicate that electroacupuncture has no significant effect on natural implantation in rats. The embryo numbers in groups M, EA', and PEA' were significantly fewer than that in group

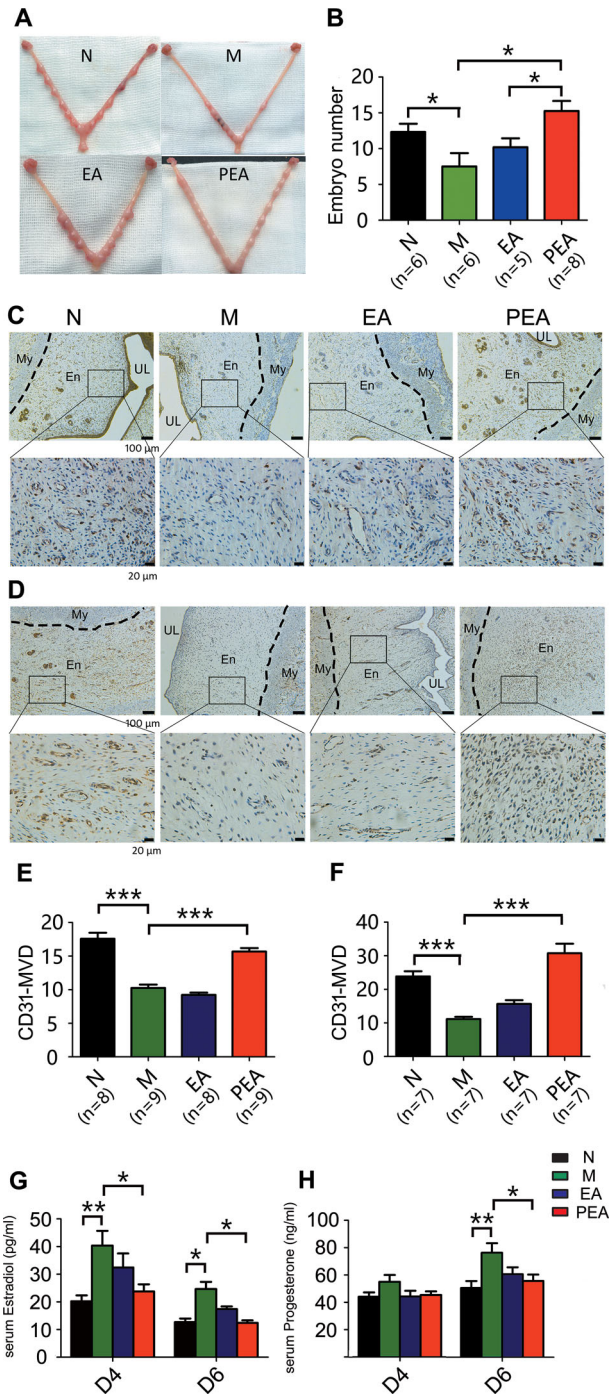

Figure 1. The effects of electroacupuncture on the embryo implantation, endometrial macrovasclar density (MVD), and serum estradiol and progesterone levels in COH rats. The implantation sites in the uteri of rats in normal (N), model (M), electroacupuncture (EA), and electroacupuncture pretreatment (PEA) groups on the eighth day (D8) of gestation (A). The embryo number in each group was counted on D8 (B). The immunohistochemistry of uterine tissue with CD31 antibodies among the four groups on the fourth day (D4) of gestation (C) and the sixth day (D6) of gestation (D). The MVD was determined in the four groups on D4 (E) and D6 (F). The levels of serum estradiol (G) and progesterone (H) in the four groups (n = 5 in each group) on D4 and D6. Data are presented as the mean ± SEM. $^*P < 0.05$, $^{**}P < 0.01$, $^{***}P < 0.001$. Magnification: 100× and 400×. UL: Uterine Lumen. My: Myometrium. En: Endometrium.

N ($P < 0.05$ or $P < 0.01$). But there were no significant differences among groups M, EA', and PEA' ($P > 0.05$, Supplementary Figure S3A and B). The MVD in group N was significantly higher than those in groups M, EA', and PEA' on D4 ($P < 0.05$) and D6 ($P < 0.001$). There were no significant differences among groups M, EA', and PEA' ($P > 0.05$, Supplementary Figure S3C–F).

The levels of serum estradiol and progesterone

In group M, the level of serum estradiol was significantly increased compared with that in group N on D4 ($P < 0.01$) and D6 ($P < 0.05$, Figure 1G). After electroacupuncture treatment, the levels of serum estradiol in groups EA and especially PEA ($P < 0.05$, Figure 1G) were decreased. The level of serum progesterone in group M was also higher compared with those in groups N, EA, and PEA. Significant differences were found between groups N and M ($P < 0.01$), and groups M and PEA ($P < 0.05$) on D6 (Figure 1H). No significant differences on the levels of serum estradiol and progesterone were seen among groups N, N+EA, and N+PEA on D4 and D6 ($P > 0.05$, Supplementary Figure S2G and H). The level of estradiol in group N was significantly lower than those in groups M, EA', and PEA' on D4 and D6 ($P < 0.01$). However, the levels of estradiol among groups M, EA', and PEA' had no remarkable differences ($P > 0.05$, Supplementary Figure S3G). Moreover, the level of progesterone in group N was significantly lower than those in groups M, EA', and PEA' on D6 ($P < 0.05$), while the levels of progesterone in groups EA' and PEA' had no significant differences with that in group M ($P > 0.05$, Supplementary Figure S3H).

VEGF-A, Angpt-1, and FGF-2 expression

Endometrial angiogenesis depends on the expression of angiogenic factors such as VEGF-A, Angpt-1, and FGF-2. The protein expression levels of VEGF-A, Angpt-1, and FGF-2 in group M were reduced compared with those in group N, except for FGF-2 expression on D4 (Figure 2A and B). However, electroacupuncture clearly upregulated the protein expression levels of VEGF-A, Angpt-1, and FGF-2 only when applied as a pretreatment (Figure 2A and B). Compared with that in group M, the relative protein expression levels of VEGF-A and Angpt-1 in groups N and PEA were significantly higher ($P < 0.05$) on D4, D6 (Figure 2C). But the expression level of FGF-2 had no significant difference among the four groups, except between groups PEA and M on D6 ($P < 0.05$; Figure 2C). However, the significant difference was not found between groups M and EA ($P > 0.05$, Figure 2C). VEGF-A mRNA expression levels were increased significantly in groups N and PEA compared with that in group M ($P < 0.05$ or $P < 0.01$ or $P < 0.001$) during peri-implantation (Figure 2D), but the FGF-2 expression levels had no significant differences among the four groups, except between groups PEA and M on D6 ($P < 0.05$; Figure 2F). The mRNA expression level of Angpt-1 was significantly lower in group M compared with that in group N on D6 ($P < 0.001$), group EA on D4 ($P < 0.05$) and group PEA on D4 ($P < 0.05$) and D6 ($P < 0.01$; Figure 2E). In all of the four groups, VEGF-A, Angpt-1, and FGF-2 are widely distributed in the rat endometrium, including the luminal and glandular epithelium, the endometrial stroma, and the vascular endothelium during the peri-implantation period (Figure 2G–I). The results above showed that the expression levels of VEGF-A, Angpt-1, FGF-2 were significantly higher in groups N and PEA than in group M, but they were not markedly increased in group EA compared with those in group M.

The percentage of DBA^+ uNK cells and expression levels of PGF and DLL-1

The percentage of DBA^+ uNK cells and the expression levels of PGF and DLL-1 changed throughout the progression of gestational development in all four groups. Prior to implantation, the percentage has no significant difference among the groups. However, after implantation, the percentage in groups N and PEA increased remarkably compared with that in group M (Figure 3A). On D4, the percentage of DBA^+ uNK cells in group N was much higher than that in groups M (Figure 3B). On D6 and D8, the percentage of DBA^+ uNK cells in groups N and PEA was significantly higher than that in group M ($P < 0.01$ or $P < 0.001$). The percentage of DBA^+ uNK cells was higher in group EA than in group M on D6 and D8, but the difference was only significant on D8 (Figure 3C and D). No significant differences in PlGF and DLL-1 protein or mRNA expression levels were found among the four groups on D4 (Figure 3E, and H–J). On D6, PGF and DLL-1 protein expression levels were increased in groups N and PEA compared with those in group M, but no remarkable differences were found between groups M and EA (Figure 3F and H). However, PGF and DLL-1 mRNA expression levels showed no significant differences among the four groups on D6 (Figure 3I and J). The protein and mRNA expression levels of PGF and DLL-1 were significantly higher in groups N and PEA than those in group M on D8 (Figure 3G, H, J).

The protein expression levels of VEGFR-2, PI3K, p-AKT, and p-ERK

The protein expression levels of VEGFR-2, PI3K, p-AKT, and p-ERK were analyzed by western blotting. VEGFR-2 protein expression was higher in groups N, EA, and, especially, PEA than that in group M on D4, D6, and, especially, D8 (Figure 4A–C). Compared with that in group M, the relative protein expression levels of VEGFR2 in groups N and PEA were significantly higher on D4, D6 ($P < 0.05$), and D8 ($P < 0.001$ or $P < 0.01$). However, the significant difference was not found between groups M and EA ($P > 0.05$, Figure 4D). The PI3K, p-AKT, and p-ERK levels showed the same trend as VEGFR-2 expression among the four groups (Figure 4A–C). The relative protein expression levels of PI3K, p-AKT, and p-ERK in groups N and PEA were remarkably higher than those in group M on D4, D6, and D8 (Figure 4E–G). Those expression levels in group EA also increased compared with those in group M, but significant differences were only found in p-AKT expression on D4 (Figure 4F).

The protein expression levels of VEGFR-2, PI3K, p-AKT, and p-ERK after siRNA injection

After intrauterine injection of siVEGFR2, the endometrial protein levels of PI3K, p-AKT, and p-ERK were all markedly reduced compared with those in endometria injected with si-NC on D4, D6, and D8 (Figure 5A). The expression of VEGFR2 was obviously silenced after VEGFR2 injection ($P < 0.01$ or $P < 0.001$, Figure 5B). The relative protein expression of PI3K, p-AKT, and p-ERK were all significantly lower in siVEGFR2-injected uteri than in siNC-injected uteri on D4, D6, and D8 ($P < 0.05$ or $P < 0.01$ or $P < 0.001$, Figure 5C–E). The results may prove that activation of the PI3K/AKT and ERK pathways has a positive relationship with VEGFR2 expression. Meanwhile, the therapeutic effect of acupuncture depends on phosphorylation of the PI3K/AKT and ERK signaling pathways.

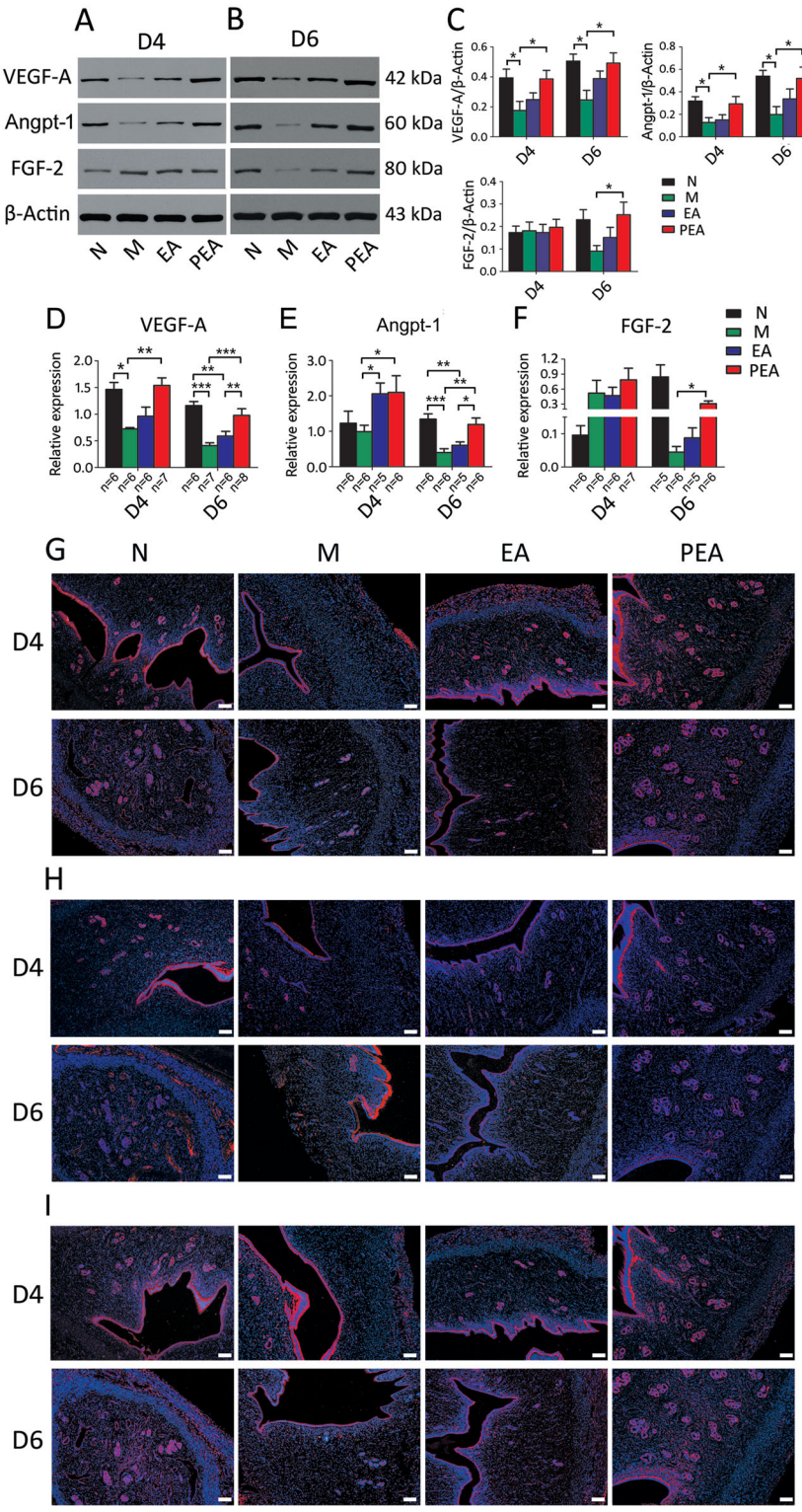

Figure 2. VEGF-A, Ang-1, and FGF-2 expression in the rat endometrium. The protein expression of VEGF-A, Angpt-1, and FGF-2 was determined by western blot in the normal (N), model (M), electroacupuncture (EA), and electroacupuncture pretreatment (PEA) groups on the fourth day (D4) (A) and sixth day (D6) (B) of gestation. The relative protein expression levels of VEGF-A, Angpt-1, FGF-2 were analyzed among the four groups (n = 3 in each group) on D4 and D6 (C). Real-time PCR was applied to analyze the relative mRNA expression levels of VEGF-A (D), Angpt-1 (E), and FGF-2 (F) among the four groups on D4 and D6. Immunofluorescence analysis of VEGF-A (G), Ang-1 (H), and FGF-2 (I) in each group on D4 and D6. Data are presented as the mean ± SEM. $^{*}P < 0.05$, $^{**}P < 0.01$, $^{***}P < 0.001$. Scale bar: 100 μm.

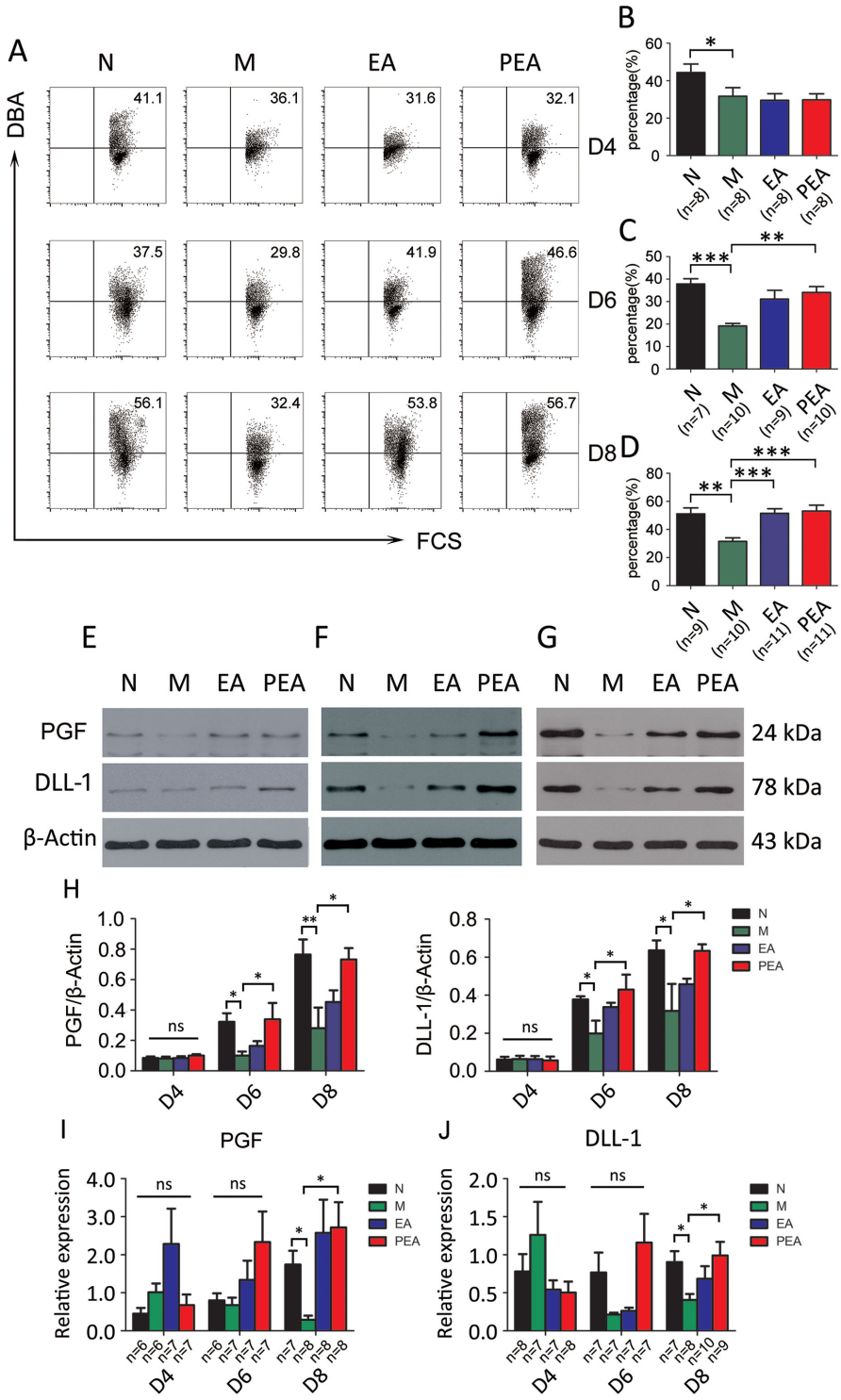

Figure 3. The percentage of DBA$^+$ uNK cells and PGF and DLL-1 expression in the endometrium. Flow cytometric analysis of the percentage of DBA$^+$ uNK cells in the normal (N), model (M), electroacupuncture (EA), and electroacupuncture pretreatment (PEA) groups on the fourth day (D4), sixth day (D6), and eighth day (D8) of gestation **(A)**. The percentage of DBA$^+$ uNK cells in each the group was counted on D4 (B), D6 (C) and D8 (D). The protein expression of PGF and DLL-1 was detected by western blot in each group on D4 (E), D6 (F), and D8 (G). The relative protein expression levels of PGF and DLL-1 were analyzed among the four groups (n=3 in each group) on D4, D6, and D8 (H). Real-time PCR was applied to analyze the relative mRNA expression of PlGF (I) and DLL-1 (J) on D4, D6, and D8. Data are presented as the mean ± SEM. $^*P < 0.05$, $^{**}P < 0.01$, $^{***}P < 0.001$.

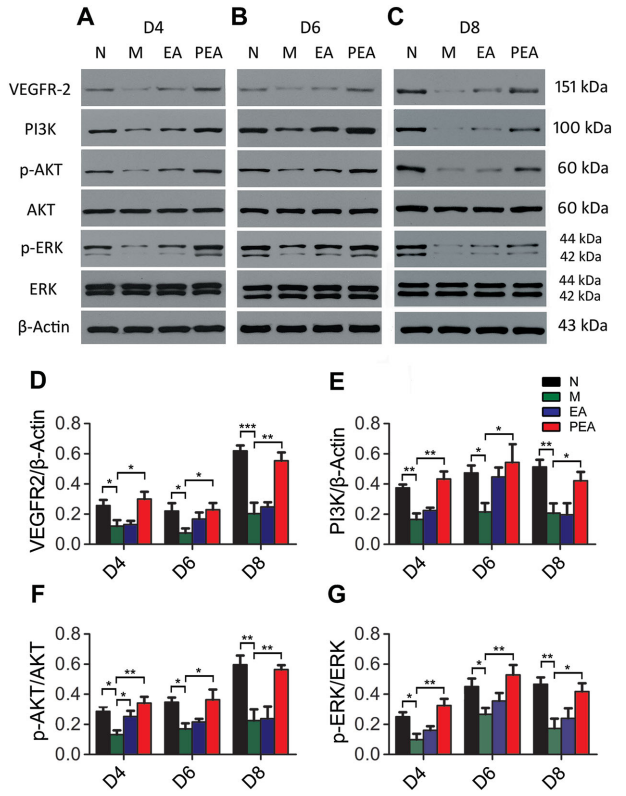

Figure 4. The protein expressions of VEGFR2, PI3K, p-AKT/AKT, and p-ERK/ERK in the endometrium. The endometrial protein levels of VEGFR2, PI3K, p-AKT/AKT, and p-ERK/ERK in the normal (N), model (M), electroacupuncture (EA), and electroacupuncture pretreatment (PEA) groups on the fourth day (D4) (A), sixth day (D6) (B), and eighth day (D8) (C) of gestation. The gray value of VEGFR2 (D), PI3K (E), p-AKT (F), and p-ERK (G) was calculated on the fourth day (D4), sixth day (D6), and eighth day (D8) of gestation (n = 3 in each group). β-Actin was used as an internal control. Data are presented as the mean ± SEM. $^{*}P < 0.05$, $^{**}P < 0.01$, $^{***}P < 0.001$.

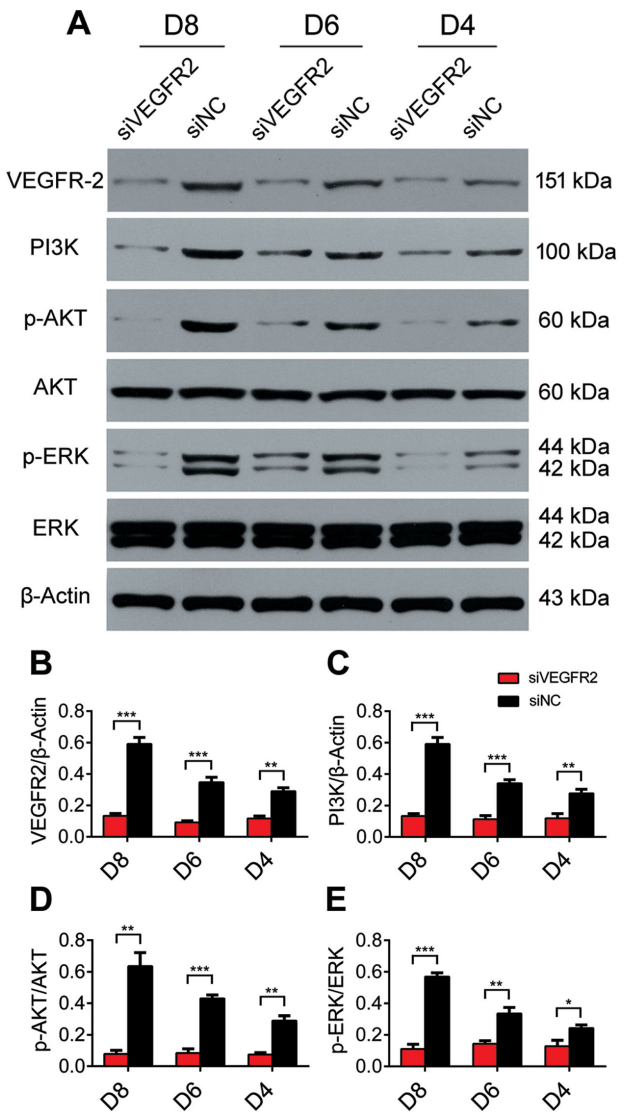

Figure 5. The protein expressions of VEGFR2, PI3K, p-AKT/AKT, and p-ERK/ERK in the endometrium after the expression of VEGFR2 was silenced. The protein levels of VEGFR2, PI3K, p-AKT/AKT, and p-ERK/ERK in the endometrium on the fourth day (D4), sixth day (D6), and eighth day (D8) of gestation after injection with si-VEGFR2 or si-NC (A). The gray value of VEGFR2 (B), PI3K (C), p-AKT (D), and p-ERK (E) was calculated on the fourth day (D4), sixth day (D6), and eighth day (D8) of gestation (n = 3 in each group). β-actin was used as an internal control. Data are presented as the mean ± SEM. $^{*}P < 0.05$, $^{**}P < 0.01$, $^{***}P < 0.001$.

Embryo number and MVD after siRNA injection

After intrauterine injection of si-VEGFR2, electroacupuncture pretreatment had no therapeutic effect on embryo implantation (Figure 6A). The embryo number was significantly lower in the siVEGFR2-injected uterus (1.88 ± 0.64) than in the siNC-injected uterus (6.63 ± 0.73; Figure 6B). There were apparently fewer CD31-positive microvessels in siVEGFR2-injected endometria than in siNC-injected endometria on D4 (Figure 6C, D, C', D'), D6 (Figure 6E, F, E', F'), and D8 (Figure 6G, H, G', H'). The MVD in siVEGFR2-injected endometria was also decreased significantly compared with that in siNC-injected endometria on D4, D6, and D8 ($P < 0.001$ or $P < 0.01$; Figure 6I–K).

Discussion

For many infertility patients, COH can be the best method to acquire enough oocytes to become pregnant. However, many studies have shown that COH has detrimental effects on endometrial receptivity by causing supraphysiological levels of serum estradiol and/or progesterone and disturbing the expression of certain genes in endometrial cells, all of which eventually result in the failure of embryo implantation [28–32]. In our study, we also found that the levels of estradiol and progesterone increased remarkably, while the embryo number decreased after COH treatment. Moreover, the premature appearance of the IW induced by supraphysiological levels of serum estradiol and/or progesterone [33, 34] influences the receptivity of the endometrium [35, 36], and impairs the synchronized development of endometrium and embryo. That is to say, after COH treatment, the IW has already closed and the process of angiogenesis slows down before the embryos are ready to implant. Hence, embryo implantation missed the best status of endometrial receptivity. After COH treatment, female rats should have produced more oocytes which means more embryos should implant in uteri compared with rats in natural pregnant cycle. However, in our study, embryo number in COH rats was fewer than that in normal rats

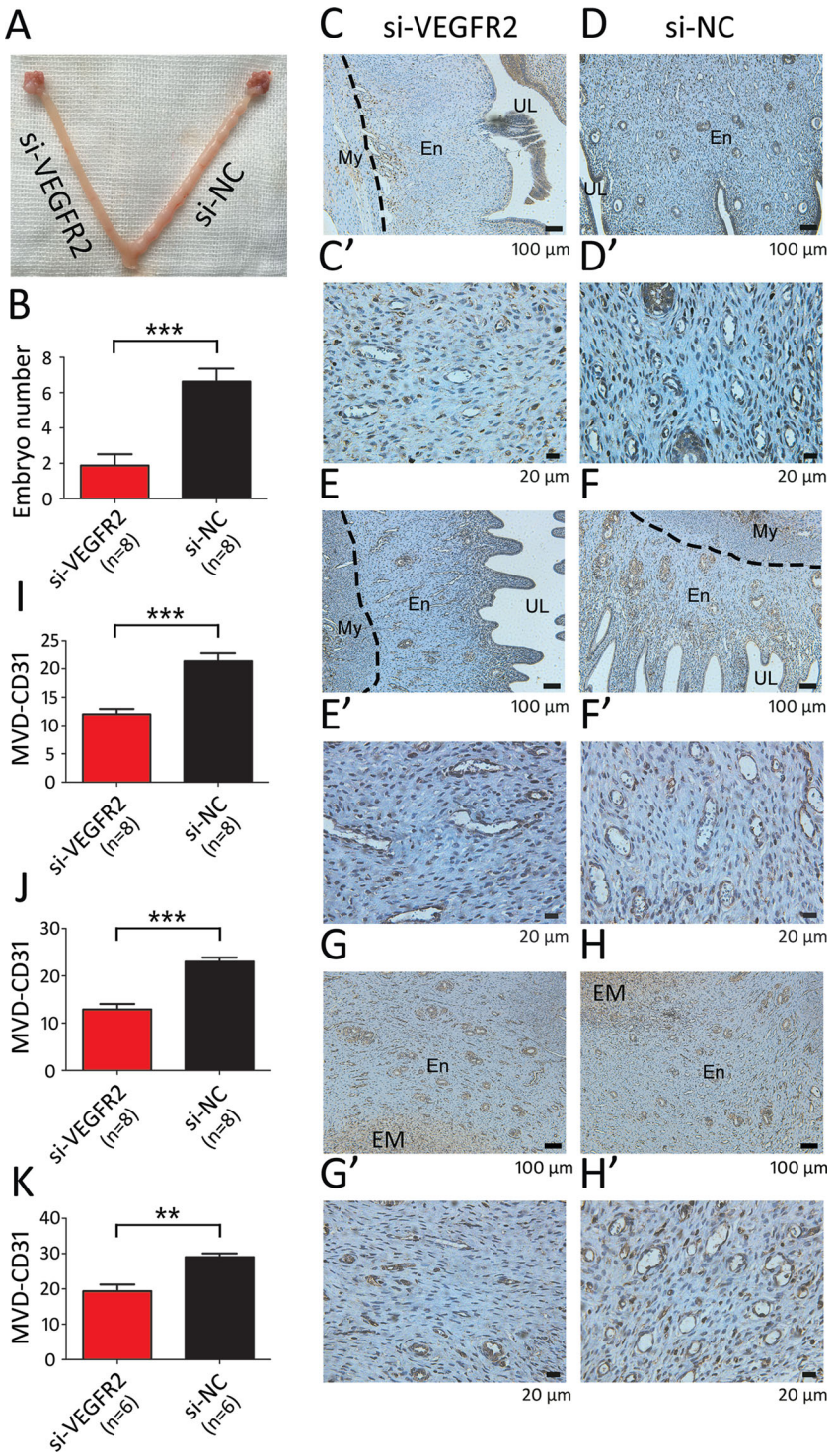

Figure 6. The effects of electroacupuncture on the embryo implantation and endometrial macrovasclar density (MVD) in COH rats after the expression of VEGFR2 was silenced. The implantation sites on the eighth day (D8) of gestation in the rat uteri injected with si-VEGFR2 or si-NC (A). The number of embryos in uteri injected with si-VEGFR2 or si-NC was counted on D8 (B). (C–H) Immunohistochemical analysis of CD31-positive vessels in the rat endometrium after injection of si-VEGFR2 or si-NC. Endometrium after injection of si-VEGFR2 or si-NC on the fourth day of gestation (D4) (C, D at 100× and C′, D′ at 400×), D6 (E, F at 100× and E′, F′ at 400×), D8 (G, H at 100× and G′, H′ at 400×). The MVD in endometrium injected with si-VEGFR2 or si-NC was determined on D4 (I), D6 (J), and D8 (K). Data are presented as the mean ± SEM. $^{*}P < 0.05$, $^{**}P < 0.01$, $^{***}P < 0.001$. Magnification: 100× and 400×. UL: Uterine Lumen. My: Myometrium. En: Endometrium. EM: Embryo.

on D8, which means that implantation rate was reduced after COH treatment. This may prove that the embryos of COH rats missed the IW, resulting in implantation failure.

As mentioned above, angiogenesis is a critical factor in determining the endometrial receptivity during the IW, and it may be impaired by the premature appearance of the IW. The regulation of angiogenesis in the endometrium involves many cytokines including the VEGF, FGF, and angiopoietin families [37, 38]. At the same time, estrogen can promote the proliferation of endothelial cells by directly bonding to the estrogen receptor on endothelial cells or other cells which have a close relationship with endothelium [39, 40]. The VEGF family includes six isoforms [37] and contains the most important cytokines that regulate angiogenesis in the endometrium [41, 42]. VEGF-A is secreted by both glandular epithelial cells and stromal cells in the endometrium and plays the most critical role in endometrial angiogenesis [37] and embryonic development [43, 44]. Angiopoietins, especially Angpt-1, play a major role in the regulation of blood vessel growth, maturation and regression, increasing the association of endothelial cells with vascular smooth muscle cells (VSMC) to remodel, stabilize, and stimulate the maturation of newly formed blood vessels [45]. Angpt-1 is expressed by VSMC and binds to its receptor Tie-2 expressed on the endothelial cells [37]. The synthesis of VEGF-A and Angpt-1 on the endometrium is induced by entrogen and ERa [46–49]. FGFs have a potential of pro-proliferation and angiogenesis, and hence might be involved in the neovascularization during the menstrual cycle and trophoblast invasion [50]. FGF-2 is mainly expressed in epithelial cells and highly mitogenic for endothelial cells which induce angiogenesis in endometrium [51]. Rat embryonic implantation is accompanied by increased expression of FGF-2 [51]. At the same time, DBA^+ uNK cells [52, 53] play an essential role in regulating decidual and placental development [54, 55] by secreting many proangiogenic cytokines such as PlGF, DLL-1, matrix metalloproteinase 2 (MMP2) and transforming growth factor beta 1 (TGFβ-1) [55, 56]. The decreased percentage of uNK cells and endometrial vascularization index provoked by COH may result in implantation failure [57].

In our present study, the endometrial MVD and the expression levels of VEGF-A, Angpt-1, and FGF-2 were all remarkably lower in COH rats than in natural cycle rats. But the level of serum estradiol increased significantly after COH treatment while the endometrial angiogenesis is poor. Although the estrogen benefits the angiogenesis, supraphysiological level of serum progesterone might oversuppress the expression of ERa in ovarian stimulation rat [1, 58] and result in the poor angiogenesis. The percentage of DBA^+ uNK cells also reduced significantly in COH rats. All these changes in COH rats resulted in a lower implantation rate during the peri-implantation period. These data indicate that the premature appearance of IW after COH treatment may disturb the synchronized development between embryo implantation and endometrial angiogenesis, resulting in poor angiogenesis during the peri-implantation period which may be one of the crucial elements causing implantation failure.

VEGFR2, as the receptor of VEGF-A, is essential for angiogenesis in the embryo implantation [59, 60] and modulates the phosphorylation of its downstream effectors, including the PI3K/AKT and ERK1/2 signaling pathways [61, 62], which play vital roles in the proliferation, survival, migration, and permeability of endothelial cells [41, 63]. Studies have found that the immunoreactivity of PI3K/AKT and ERK signaling pathways are increased during the implantation period [64] and that angiogenesis can be inhibited by downregulating the PI3K/AKT and ERK signaling pathways [65]. Furthermore, in the present study, the VEGFR2-induced PI3K/AKT and ERK signaling pathways were also affected by COH, which may indicate that the poor angiogenesis in COH rats was caused by decreased phosphorylation of AKT and ERK.

According to the theory of Traditional Chinese Medicine, acupuncture points are special locations on meridian networks that are thought to be channels where “qi” and “blood” circulate. Certain acupoints have specific therapeutic effects. In this study, SP6 and ST36 were selected as the stimulated points. SP6 is considered a classic acupoint for curing gynecological diseases, while ST36 can facilitate the production of “qi” and “blood” and promote patient rehabilitation [66]. Hence, in the present study, we attempted to improve endometrial receptivity and increase the implantation rate by administering electroacupuncture treatment. Our previous research found that Cx43 is involved in the acupuncture effect of improving rat blastocyst implantation [19]. The attenuated expression of CCL2 and CXCL8 which was induced by mifepristone treatment could be markedly reversed by acupuncture which finally improved embryo implantation [18]. Another research demonstrated that the levels of TNF-α and MCP-1 in serum and of IL-6 in ovary which are all associated with OHSS were significantly rescued by electroacupuncture [67]. In the present study, we found that when SP6 and ST36 were chosen as stimulated points, not only implantation rate was significantly improved, but serum estradiol and progesterone levels also remarkably decreased in COH rats. So, we speculate that electroacupuncture may influence the function of hypothalamic-pituitary-gonadal axis which regulates the secretion of estrogen and progesterone, and then facilitate the endometrial angiogenesis. At the same time, we randomly chose another two acupoints, PC6 and TE5, as a control treatment. And we found that when PC6 and TE5 were selected as stimulated points, electroacupuncture treatment could not facilitate embryo implantation in rats. Obviously, electroacupuncture in SP6 combined with ST36 is a better strategy in improving implantation rate in COH rats.

Our study showed that electroacupuncture pretreatment facilitates the expression of VEGFR2 and increases the phosphorylation of AKT and ERK. And electroacupuncture pretreatment, maybe in this way, enhances endometrial angiogenesis and increases the implantation rate in COH rats. However, electroacupuncture pretreatment lost its therapeutic effect when VEGFR2 expression was silenced with siVEGFR2. Thus, electroacupuncture pretreatment can improve implantation mainly through the VEGFR2/PI3K/AKT and VEGFR2/ERK signaling pathways. Furthermore, our study also showed that electroacupuncture treatment was administered prior to COH rather than after it can obtain a better therapeutic effect.

There are some limitations in our study. First, rats were pretreated with acupuncture for only 3 days before PMSG injection. Therefore, a more appropriate therapeutic course still needs to be investigated in clinical trial. Second, we chose only SP6+ST36 and PC6+TE5 as the acupoints. There may be additional and better acupoints to improve angiogenesis in COH rats.

In conclusion, our present study supports that electroacupuncture treatment can facilitate embryo implantation and improve endometrial angiogenesis during peri-implantation period by increasing the expression of VEGFR2/PI3K/AKT and VEGFR2/ERK signaling pathways in COH rats. Meanwhile, electroacupuncture had a superior therapeutic effect when initiated as a pretreatment. Electroacupuncture, especially when administered as a pretreatment, may represent a simple and effective therapeutic strategy for improving the implantation rate in IVF-ET.

Supplementary data

Supplementary data are available at *BIOLRE* online.

Supplementary Figure S1. The effect of anesthesia with isoflurane on embryo implantation in rats. The implantation sites in the uteri of rats in the groups N and N+Anesthesia on the eighth day (D8) of gestation (A). The embryo number in each of the two groups was counted on D8 (B). The implantation sites in the uteri of rats in the groups M and M+Anesthesia on D8 (C). The embryo number in each of the two groups was counted on D8 (D). n = 5 in each group. Data are presented as the mean ± SEM.

Supplementary Figure S2. The effects of electroacupuncture on the embryo implantation, endometrial macrovasclar density (MVD), and serum estradiol and progesterone levels in normal pregnant rats. The implantation sites in the uteri of rats in normal (N), normal+electroacupuncture (N+EA), normal+electroacupuncture pretreatment (N+PEA) groups on the eighth day (D8) of gestation (A). The embryo number in each group was counted on D8 (B). The immunohistochemistry of uterine tissue with CD31 antibodies among the three groups on the fourth day (D4) of gestation (C) and the sixth day (D6) of gestation (E). The MVD was determined in the three groups on D4 (D) and D6 (F). The levels of serum estradiol (G) and progesterone (H) in the three groups on D4 and D6 (n = 5 in each group). Data are presented as the mean ± SEM. Magnification: 100×and 400×. UL: Uterine Lumen. My: Myometrium. En: Endometrium.

Supplementary Figure S3. The effects of electroacupuncture on the embryo implantation, endometrial macrovasclar density (MVD), and serum estradiol and progesterone levels when PC6 and TE5 were chosen as acupoints. The implantation sites in the uteri of rats in normal (N), model (M), electroacupuncture control (EA'), and electroacupuncture pretreatment control (PEA') groups on the eighth day (D8) of gestation (A). The embryo number in each group was counted on D8 (B). The immunohistochemistry of uterine tissue with CD31 antibodies among the four groups on the fourth day (D4) of gestation (C) and the sixth day (D6) of gestation (D). The MVD was determined in the four groups on D4 (E) and D6 (F). The levels of serum estradiol (G) and progesterone (H) in the four groups on D4 and D6 (n = 5 in each group). Data are presented as the mean ± SEM. $^{*}P < 0.05$, $^{**}P < 0.01$, $^{***}P < 0.001$. Magnification: 100× and 400×. UL: Uterine Lumen. My: Myometrium. En: Endometrium.

Supplementary Table S1. The real-time PCR primer sequences.

Supplementary Table S2. Antibody Table.

Acknowledgments

Author Contributions: GH and WY designed the experiments and revised the manuscript. WC designed part of the experiments, carried out the experiments, analyzed the data, and drafted the manuscript. JC helped to finish the biochemical and immunological experiments. MX, ZZ, and QZ helped to carry out the animal experiments.

Conflict of Interest: The authors have declared that no conflict of interest exists.

References

1. Fu H, Sun J, Tan Y, Zhou H, Xu W, Zhou J, Chen D, Zhang C, Zhu X, Zhang Y, Wu X, Xi Z. Effects of acupuncture on the levels of serum estradiol and pituitary estrogen receptor beta in a rat model of induced super ovulation. *Life Sci* 2018; **197**:109–113.
2. Deng S, Xu J, Zeng J, Hu L, Wu Y. Ovarian stimulation leads to a severe implantation defect in mice. *Reprod Biomed Online* 2013; **27**:172–175.
3. Ezoe K, Daikoku T, Yabuuchi A, Murata N, Kawano H, Abe T, Okuno T, Kobayashi T, Kato K. Ovarian stimulation using human chorionic gonadotrophin impairs blastocyst implantation and decidualization by altering ovarian hormone levels and downstream signaling in mice. *Mol Hum Reprod* 2014; **20**:1101–1116.
4. Lindsay LA, Murphy CR. Ovarian hyperstimulation affects fluid transporters in the uterus: a potential mechanism in uterine receptivity. *Reprod Fertil Dev* 2014; **26**:982–990.
5. Son WY, Chung JT, Das M, Buckett W, Demirtas E, Holzer H. Fertilization, embryo development, and clinical outcome of immature oocytes obtained from natural cycle in vitro fertilization. *J Assist Reprod Genet* 2013; **30**:43–47.
6. Ghaffari F, Sadatmahalleh SJ, Akhoond MR, Eftekhari Yazdi P, Zolfaghari Z. Evaluating the effective factors in pregnancy after intrauterine insemination: a retrospective study. *Int J Fertil Steril* 2015; **9**:300–308.
7. Kara M, Kutlu T, Sofuoglu K, Devranoglu B, Cetinkaya T. Association between serum estradiol level on the hCG administration day and IVF-ICSI outcome. *Iranian J Reprod Med* 2012; **10**:53–58.
8. Zhang W, Xiao X, Zhang J, Wang W, Wu J, Peng L, Wang X. Clinical outcomes of frozen embryo versus fresh embryo transfer following in vitro fertilization: a meta-analysis of randomized controlled trials. *Arch Gynecol Obstet* 2018; **298**:259–272.
9. Teh WT, McBain J, Rogers P. What is the contribution of embryo-endometrial asynchrony to implantation failure? *J Assist Reprod Genet* 2016; **33**:259–272.
10. Valdes CT, Schutt A, Simon C. Implantation failure of endometrial origin: it is not pathology, but our failure to synchronize the developing embryo with a receptive endometrium. *Fertil Steril* 2017; **108**:15–18.
11. Evans J, Hannan NJ, Hincks C, Rombauts LJ, Salamonsen LA. Defective soil for a fertile seed? Altered endometrial development is detrimental to pregnancy success. *PLoS One* 2012; **7**:e53098.
12. Karizbodagh MP, Rashidi B, Sahebkar A, Masoudifar A, Mirzaei H. Implantation window and angiogenesis. *J Cell Biochem* 2017; **118**:4141–4151.
13. Klauber N, Rohan RM, Flynn E, D'Amato RJ. Critical components of the female reproductive pathway are suppressed by the angiogenesis inhibitor AGM-1470. *Nat Med* 1997; **3**:443–446.
14. Meduri G, Bausero P, Perrot-Applanat M. Expression of vascular endothelial growth factor receptors in the human endometrium: modulation during the menstrual cycle. *Biol Reprod* 2000; **62**:439–447.
15. Gong X, Tong Q, Chen Z, Zhang Y, Xu C, Jin Z. Microvascular density and vascular endothelial growth factor and osteopontin expression during the implantation window in a controlled ovarian hyperstimulation rat model. *Exp Ther Med* 2015; **9**:773–779.
16. Carson DD, Bagchi I, Dey SK, Enders AC, Fazleabas AT, Lessey BA, Yoshinaga K. Embryo implantation. *Dev Biol* 2000; **223**:217–237.
17. Gui J, Xiong F, Yang W, Li J, Huang G. Effects of acupuncture on LIF and IL-12 in rats of implantation failure. *Am J Reprod Immunol* 2012; **67**:383–390.
18. Gao W, Tang X, Chen Z, Guo Y, Wang L, Zhang M, Huang G. Effects of acupuncture on CCL2 and CXCL8 expression and the subset of uNK cells in rats with embryo implantation failure. *Evid Based Comp Alter Med* 2013; **2013**:1–12.
19. Huang GY, Zheng CH, Wu YX, Wang W. Involvement of connexin 43 in the acupuncture effect of improving rat blastocyst implantation. *Fertil Steril* 2010; **93**:1715–1717.
20. Shuai Z, Lian F, Li P, Yang W. Effect of transcutaneous electrical acupuncture point stimulation on endometrial receptivity in women undergoing frozen-thawed embryo transfer: a single-blind prospective randomised controlled trial. *Acupunct Med* 2015; **33**:9–15.
21. Qu F, Wang FF, Wu Y, Zhou J, Robinson N, Hardiman PJ, Pan JX, He YJ, Zhu YH, Wang HZ, Ye XQ, He KL et al. Transcutaneous electrical Acupoint stimulation improves the outcomes of in vitro fertilization: a prospective, randomized and controlled study. *Explore* 2017; **13**:306–312.

22. Ma S, Li D, Feng Y, Jiang J, Shen B. Effects of electroacupuncture on uterine morphology and expression of oestrogen receptors in ovariectomised rats. *Acupunct Med* 2017; **35**:208–214.
23. Groppetti D, Pecile AM, Sacerdote P, Bronzo V, Ravasio G. Effectiveness of electroacupuncture analgesia compared with opioid administration in a dog model: a pilot study. *Br J Anaesth* 2011; **107**:612–618.
24. Johansson J, Feng Y, Shao R, Lonn M, Billig H, Stener-Victorin E. Intense electroacupuncture normalizes insulin sensitivity, increases muscle GLUT4 content, and improves lipid profile in a rat model of polycystic ovary syndrome. *Am J Physiol Endocrinol Metab* 2010; **299**:E551–E559.
25. Manneras L, Jonsdottir IH, Holmang A, Lonn M, Stener-Victorin E. Low-frequency electro-acupuncture and physical exercise improve metabolic disturbances and modulate gene expression in adipose tissue in rats with dihydrotestosterone-induced polycystic ovary syndrome. *Endocrinology* 2008; **149**:3559–3568.
26. Xu B, Geerts D, Bu Z, Ai J, Jin L, Li Y, Zhang H, Zhu G. Regulation of endometrial receptivity by the highly expressed HOXA9, HOXA11 and HOXD10 HOX-class homeobox genes. *Hum Reprod* 2014; **29**:781–790.
27. Norton WB, Scavizzi F, Smith CN, Dong W, Raspa M, Parker-Thornburg JV. Refinements for embryo implantation surgery in the mouse: comparison of injectable and inhalant anesthesias - tribromoethanol, ketamine and isoflurane - on pregnancy and pup survival. *Lab Anim* 2016; **50**:335–343.
28. Haouzi D, Assou S, Dechanet C, Anahory T, Dechaud H, De Vos J, Hamamah S. Controlled ovarian Hyperstimulation for in vitro fertilization alters endometrial receptivity in humans: protocol effects. *Biol Reprod* 2010; **82**:679–686.
29. Horcajadas JA, Riesewijk A, Polman J, van Os R, Pellicer A, Mosselman S, Simon C. Effect of controlled ovarian hyperstimulation in IVF on endometrial gene expression profiles. *Mol Hum Reprod* 2004; **11**:195–205.
30. Liu Y, Lee KF, Ng EH, Yeung WS, Ho PC. Gene expression profiling of human peri-implantation endometria between natural and stimulated cycles. *Fertil Steril* 2008; **90**:2152–2164.
31. Mirkin S, Nikas G, Hsiu JG, Diaz J, Oehninger S. Gene expression profiles and structural/functional features of the peri-implantation endometrium in natural and gonadotropin-stimulated cycles. *J Clin Endocrinol Metab* 2004; **89**:5742–5752.
32. Xiong Y, Wang J, Liu L, Chen X, Xu H, Li TC, Wang CC, Zhang S. Effects of high progesterone level on the day of human chorionic gonadotrophin administration in in vitro fertilization cycles on epigenetic modification of endometrium in the peri-implantation period. *Fertil Steril* 2017; **108**:269.e1–276.e1.
33. Nikas G, Develioglu OH, Toner JP, Jones HW, Jr. Endometrial pinopodes indicate a shift in the window of receptivity in IVF cycles. *Hum Reprod* 1999; **14**:787–792.
34. Kolb BA, Paulson RJ. The luteal phase of cycles utilizing controlled ovarian hyperstimulation and the possible impact of this hyperstimulation on embryo implantation. *Am J Obstet Gynecol* 1997; **176**:1262–1269; discussion 1267–1269.
35. Simon C, Mercader A, Frances A, Gimeno MJ, Polan ML, Remohi J, Pellicer A. Hormonal regulation of serum and endometrial IL-1alpha, IL-1beta and IL-1ra: IL-1 endometrial microenvironment of the human embryo at the apposition phase under physiological and supraphysiological steroid level conditions. *J Reprod Immunol* 1996; **31**:165–184.
36. Valbuena D, Martin J, de Pablo JL, Remohi J, Pellicer A, Simon C. Increasing levels of estradiol are deleterious to embryonic implantation because they directly affect the embryo. *Fertil Steril* 2001; **76**:962–968.
37. Smith SK. Regulation of angiogenesis in the endometrium. *Trends Endocrinol Metab* 2001; **12**:147–151.
38. Rizov M, Andreeva P, Dimova I. Molecular regulation and role of angiogenesis in reproduction. *Taiwanese J Obstet Gynecol* 2017; **56**:127–132.
39. Mueller MD, Vigne JL, Minchenko A, Lebovic DI, Leitman DC, Taylor RN. Regulation of vascular endothelial growth factor (VEGF) gene transcription by estrogen receptors alpha and beta. *Proc Natl Acad Sci* 2000; **97**:10972–10977.
40. Totonchi H, Miladpour B, Mostafavi-Pour Z, Khademi F, Kasraeian M, Zal F. Quantitative analysis of expression level of estrogen and progesterone receptors and VEGF genes in human endometrial stromal cells after treatment with nicotine. *Toxicol Mech Methods* 2016; **26**:595–600.
41. Ha CH, Bennett AM, Jin ZG. A novel role of vascular endothelial cadherin in modulating c-Src activation and downstream signaling of vascular endothelial growth factor. *J Biol Chem* 2008; **283**:7261–7270.
42. Tan W, Chen L, Guo L, Ou X, Xie D, Quan S. Relationship between macrophages in mouse uteri and angiogenesis in endometrium during the peri-implantation period. *Theriogenology* 2014; **82**:1021–1027.
43. Carmeliet P, Ferreira V, Breier G, Pollefeyt S, Kieckens L, Gertsenstein M, Fahrig M, Vandenhoeck A, Harpal K, Eberhardt C, Declercq C, Pawling J et al. Abnormal blood vessel development and lethality in embryos lacking a single VEGF allele. *Nature* 1996; **380**:435–439.
44. Ferrara N, Carver-Moore K, Chen H, Dowd M, Lu L, O'Shea KS, Powell-Braxton L, Hillan KJ, Moore MW. Heterozygous embryonic lethality induced by targeted inactivation of the VEGF gene. *Nature* 1996; **380**:439–442.
45. Tsuzuki T, Okada H, Cho H, Shimoi K, Miyashiro H, Yasuda K, Kanzaki H. Divergent regulation of angiopoietin-1, angiopoietin-2, and vascular endothelial growth factor by hypoxia and female sex steroids in human endometrial stromal cells. *European J Obstet Gynecol Reprod Biol* 2013; **168**:95–101.
46. Nayak NR, Brenner RM. Vascular proliferation and vascular endothelial growth factor expression in the rhesus macaque endometrium. *J Clin Endocrinol Metab* 2002; **87**:1845–1855.
47. Niklaus AL, Aberdeen GW, Babischkin JS, Pepe GJ, Albrecht ED. Effect of estrogen on vascular endothelial Growth/Permeability factor expression by glandular epithelial and stromal cells in the baboon endometrium. *Biol Reprod* 2003; **68**:1997–2004.
48. Shifren JL, Tseng JF, Zaloudek CJ, Ryan IP, Meng YG, Ferrara N, Jaffe RB, Taylor RN. Ovarian steroid regulation of vascular endothelial growth factor in the human endometrium: implications for angiogenesis during the menstrual cycle and in the pathogenesis of endometriosis. *J Clin Endocrinol Metab* 1996; **81**:3112–3118.
49. Bonagura TW, Aberdeen GW, Babischkin JS, Koos RD, Pepe GJ, Albrecht ED. Divergent regulation of angiopoietin-1 and -2, Tie-2, and thrombospondin-1 expression by estrogen in the baboon endometrium. *Mol Reprod Dev* 2010; **77**:430–438.
50. Quinn CE, Casper RF. Pinopodes: a questionable role in endometrial receptivity. *Hum Reprod Update* 2009; **15**:229–236.
51. Kim SM, Kim JS. A review of mechanisms of implantation. *Dev Reprod* 2017; **21**:351–359.
52. Chen Z, Zhang J, Hatta K, Lima PD, Yadi H, Colucci F, Yamada AT, Croy BA. DBA-Lectin reactivity defines mouse uterine natural killer cell subsets with biased gene expression. *Biol Reprod* 2012; **87**:81.
53. Paffaro VA, Bizinotto MC, Joazeiro PP, Yamada AT. Subset classification of mouse uterine natural killer cells by DBA lectin reactivity. *Placenta* 2003; **24**:479–488.
54. Chakraborty D, Rumi MA, Konno T, Soares MJ. Natural killer cells direct hemochorial placentation by regulating hypoxia-inducible factor dependent trophoblast lineage decisions. *Proc Natl Acad Sci* 2011; **108**:16295–16300.
55. Ratsep MT, Felker AM, Kay VR, Tolusso L, Hofmann AP, Croy BA. Uterine natural killer cells: supervisors of vasculature construction in early decidua basalis. *Reproduction* 2014; **149**:R91–R102.
56. Thiruchelvam U, Wingfield M, O'Farrelly C. Natural killer cells: Key players in endometriosis. *Am J Reprod Immunol* 2015; **74**:291–301.
57. Junovich G, Mayer Y, Azpiroz A, Daher S, Iglesias A, Zylverstein C, Gentile T, Pasqualini S, Markert UR, Gutierrez G. Ovarian stimulation affects the levels of regulatory endometrial NK cells and angiogenic cytokine VEGF. *Am J Reprod Immunol* 2011; **65**:146–153.
58. Halasz M, Szekeres-Bartho J. The role of progesterone in implantation and trophoblast invasion. *J Reprod Immunol* 2013; **97**:43–50.
59. Wollenhaupt K, Welter H, Einspanier R, Manabe N, Brussow KP. Expression of epidermal growth factor receptor (EGF-R), vascular endothelial growth factor receptor (VEGF-R) and fibroblast growth factor receptor (FGF-R) systems in porcine oviduct and endometrium during the time of implantation. *J Reprod Dev* 2004; **50**:269–278.

60. Shalaby F, Rossant J, Yamaguchi TP, Gertsenstein M, Wu XF, Breitman ML, Schuh AC. Failure of blood-island formation and vasculogenesis in Flk-1-deficient mice. *Nature* 1995; **376**:62–66.
61. Corti F, Simons M. Modulation of VEGF receptor 2 signaling by protein phosphatases. *Pharmacol Res* 2017; **115**:107–123.
62. Hofer E, Schweighofer B. Signal transduction induced in endothelial cells by growth factor receptors involved in angiogenesis. *Thromb Haemost* 2007; **97**:355–363.
63. Olsson AK, Dimberg A, Kreuger J, Claesson-Welsh L. VEGF receptor signalling -in control of vascular function. *Nat Rev Mol Cell Biol* 2006; **7**:359–371.
64. Ekizceli G, Inan S, Oktem G, Onur E, Ozbilgin K. Assessment of mTOR pathway molecules during implantation in rats. *Biotechnic Histochem* 2017; **92**:450–458.
65. Dai F, Gao L, Zhao Y, Wang C, Xie S. Farrerol inhibited angiogenesis through Akt/mTOR, Erk and Jak2/Stat3 signal pathway. *Phytomedicine* 2016; **23**:686–693.
66. Wang Q. *Science of Acumox Therapeutics*. Beijing: China Press of Traditional Chinese Medicine; 2003: 154.
67. Chen L, Sun HX, Xia YB, Sui LC, Zhou J, Huang X, Zhou JW, Shao YD, Shen T, Sun Q, Liang YJ, Yao B. Electroacupuncture decreases the progression of ovarian hyperstimulation syndrome in a rat model. *Reprod Biomed Online* 2016; **32**:538–544.